Sphingosine-1-phosphate receptor 1 enhances olfactory receptor 51E1-mediated inhibition of proliferation via Src/JNK signaling in prostate cancer cells

KIHEON KIM[1], JINWOO LEE[1], CHULWON CHOI[1], JUNGNAM BAE[1], HEE-JUNG CHOI[1] and WON-KI HUH[1-3]

[1]Department of Biological Sciences, Seoul National University, Seoul 08826, Republic of Korea; [2]GPCR Therapeutics, Gwanak, Seoul 08790, Republic of Korea; [3]Institute of Biodiversity, Seoul National University, Seoul 08826, Republic of Korea

Received September 24, 2025; Accepted February 18, 2026

DOI: 10.3892/or.2026.9103

Abstract. Olfactory receptors (ORs) are ectopically expressed in multiple cancers and can regulate tumor cell behavior, yet their clinical relevance and regulatory mechanisms remain poorly defined. OR51E1 is highly expressed in prostate cancer (PC) and suppresses tumor cell proliferation upon activation, but its expression alone does not correlate with patient prognosis, suggesting additional regulatory factors. Using transcriptomic analyses of The Cancer Genome Atlas and Genotype-Tissue Expression datasets, functional screening of G-protein-coupled receptors, and mechanistic studies in PC cells, sphingosine-1-phosphate receptor 1 (S1PR1) was identified as a key modulator of OR51E1 function. Activation of OR51E1 by nonanoic acid (NA) or butyric acid reduced PC cell survival in an OR51E1-dependent manner, and this effect was abolished in OR51E1 knockout cells. S1PR1 enhanced OR51E1-mediated signaling by increasing its surface expression and amplifying downstream apoptotic responses. Although OR51E1 activation induced cAMP signaling, NA-induced cytotoxicity was independent of the canonical Gs/olf-cAMP pathway and instead required Src and JNK activation, which was further potentiated by S1PR1. Clinically, co-expression of OR51E1 and S1PR1 was significantly associated with improved progression-free interval in patients with prostate adenocarcinoma, particularly in stage II disease, whereas OR51E1 expression alone showed no prognostic value. Collectively, these findings define a previously unrecognized OR51E1-S1PR1 signaling axis that suppresses PC cell survival through Src/JNK-dependent mechanisms and highlight GPCR-mediated regulation of ectopic olfactory receptors as a determinant of tumor behavior and patient outcome.

Correspondence to: Professor Won-Ki Huh, Department of Biological Sciences, Seoul National University, 1 Gwanak, Gwanak, Seoul 08826, Republic of Korea
E-mail: wkh@snu.ac.kr

Abbreviations: BA, butyric acid; CCK-8, Cell Counting Kit-8; DRD2, dopamine receptor D2; FBS, fetal bovine serum; Golf, olfactory Gα protein; GPCR, G-protein-coupled receptor; NA, nonanoic acid; OR, olfactory receptor; OR51E1, olfactory receptor 51E1; PRAD, prostate adenocarcinoma; S1PR1, sphingosine-1-phosphate receptor 1; TCGA, The Cancer Genome Atlas; TPM, transcripts per million

Key words: OR51E1, S1PR1, prostate cancer, tumor suppression, apoptosis, JNK pathway

Introduction

Olfactory receptors (ORs) constitute the largest family of G-protein-coupled receptors (GPCRs), accounting for ~400 and 1,200 intact genes in humans and mice, respectively (1-3). In olfactory sensory neurons, activation of ORs triggers dissociation of the olfactory Gα protein (Golf) from its Gβγ subunit, followed by activation of type III adenylyl cyclase and an increase in intracellular cAMP. Elevated cAMP levels induce the opening of cAMP-gated Ca^{2+} channels, which in turn trigger membrane depolarization and the generation of action potentials (4-7).

Most ORs are expressed in the nasal olfactory epithelium, but accumulating evidence indicates that they are also present in various non-nasal tissues (8,9). This ectopic expression suggests potential roles for ORs beyond smell perception, mediating diverse physiological processes (10-15). For example, OR17-4 is expressed in human spermatozoa and plays an essential role in efficient fertilization by mediating sperm chemotaxis toward the oocyte (10-12). The mouse olfactory receptor MOR23 (a homolog of human OR10J5) has been shown to promote skeletal muscle regeneration by regulating myoblast adhesion and migration, underscoring the role of ORs in tissue remodeling and repair (13). OR78 in renal juxtaglomerular cells responds to short-chain fatty acids derived from gut microbiota, linking microbial signals to renin secretion and systemic blood pressure regulation (14). In the liver, OR10J5 senses the plant-derived compound α-cedrene and regulates hepatic lipid metabolism and steatosis through the cAMP-PKA signaling pathway, suggesting a metabolic role for ORs in energy homeostasis (15).

Notably, studies have reported that ORs are abnormally expressed in various tumor cells, including those in breast cancer (16), melanoma (17), colon cancer (18), bladder cancer (19), neuroendocrine carcinomas (20), liver cancer (21), lung cancer (22) and brain cancer (23). In these cancers, ORs can regulate cell invasion, migration, proliferation and apoptosis through their own signaling cascades involving both canonical and non-canonical signaling pathways (24). Olfactory receptor 51E1 (OR51E1) is one of the most abundantly expressed ectopic ORs in various tissues, including small intestine neuroendocrine carcinoma (25,26), lung carcinoid (27) and prostate carcinoma (24,28-30). Because OR51E1 is highly expressed in prostate tissues, it has also been referred to as prostate-specific GPCR2 (28). Interestingly, OR51E1 gene expression is significantly higher in prostate cancer (PC) tissues than in normal prostate tissues (28-30), although no correlation between OR51E1 expression and survival of patients with PC has been identified. Furthermore, studies have shown that activation of OR51E1 by short- and medium-chain fatty acid ligands, such as butyrate, triggers intracellular signaling cascades characterized by elevated cAMP levels and PKA activation. This signaling promotes the upregulation of cell cycle inhibitors, including p21 and p27, as well as the tumor suppressor p53, leading to cell cycle arrest (29,30). However, the precise molecular mechanisms underlying these effects remain to be fully elucidated.

In the present study, the expression and prognostic significance of OR51E1 and other GPCRs in PC were analyzed. Using nonanoic acid (NA)-induced cAMP production as a functional readout, we found that sphingosine-1-phosphate receptor 1 (S1PR1) can regulate OR51E1-mediated signaling and tumor suppression. The present findings provide mechanistic insights into the tumor-suppressive effects of OR51E1 in PC and suggest the existence of specific GPCR-mediated regulatory mechanisms for ectopic olfactory receptors.

Materials and methods

Cell culture and reagents. LNCaP cells were obtained from the Korean Cell Line Bank, and Du145 and PC3 cells were purchased from the American Type Culture Collection. LNCaP, DU145 and PC3 cells were cultured in RPMI-1640 medium supplemented with 10% fetal bovine serum (FBS; Hyclone; Cytiva), 100 U/ml penicillin, 100 μg/ml streptomycin, and 20 mM HEPES at 37˚C in a humidified 5% CO_2 incubator. Hana3A cells, generously provided by Professor Hiroaki Matsunami (Duke University School of Medicine), were cultured in Dulbecco's modified Eagle's medium supplemented with 10% FBS, penicillin and streptomycin. Butyric acid (BA) and NA were purchased from MilliporeSigma. TC-G1006 (cat. no. 4747) was purchased from Tocris Bioscience. Anti-S1PR1 (cat. no. 55133-1-AP) and anti-PARP1 (cat. no. 51-6639GR) antibodies were purchased from Proteintech Group, Inc. and BD Biosciences, respectively. Anti-ERK1/2 (cat. no. 9102), anti-phospho-ERK1/2 (T202/Y204) (cat. no. 4370), anti-SRC (cat. no. 2109), anti-phospho-SRC (Tyr416; cat. no. 6943), anti-JNK (cat. no. 9252), anti-phospho-JNK (T183/Y185; cat. no. 4668), anti-p38 MAPK (cat. no. 8690) and anti-phospho-p38 MAPK (T180/Y182; cat. no. 4511) antibodies were purchased from Cell Signaling Technology, Inc. Anti-β-Actin-HRP (cat. no. sc-47778) and anti-rabbit IgG HRP-conjugated (cat. no. AS014) antibodies were purchased from Santa Cruz Biotechnology, Inc. and ABclonal Biotech Co., Ltd., respectively.

Plasmids. Human GPCR cDNAs were obtained from the Missouri S&T cDNA Resource Center and cloned into pENTR/D-TOPO vectors (Invitrogen; Thermo Fisher Scientific, Inc.) as previously described (31). If necessary, a stop codon was introduced via site-directed mutagenesis. N-terminal lucy-flag-rho tag of OR51E1 was a kind gift from Jennifer L. Pluznick (32). Flag, and Myc tags were cloned at the N-terminus of each GPCR using one-step sequence- and ligation-independent cloning (33). GPCRs were subcloned into pcDNA3.1 or pLenti-CMV-Puro-DEST (Addgene, Inc.; cat. no. 17452; a gift from Eric Campeau & Paul Kaufman) vectors using the Gateway cloning system (Invitrogen; Thermo Fisher Scientific, Inc.), following the manufacturer's instructions. pGL4.29[luc2P/CRE/Hygro] reporter plasmid was purchased from Promega Corporation (cat. no. E8471). GloSensor-22F plasmid was purchased from Promega Corporation (cat. no. E2301) for measuring cAMP production. For CRISPR-Cas9 gene editing, non-targeting control sgRNA and guide RNAs targeting OR51E1 were designed using the OmniGuide RNA Design Tool (GenScript; https://www.genscript.com/tools/gRNA-design-tool) and were cloned into the lentiCRISPR-v2 vector (Addgene, Inc.; cat. no. 52961; a gift from Feng Zhang).

Generation of stably transduced cells using lentivirus. Lentiviral particles were produced using the ViraPower Lentiviral Expression System (cat. no. K4960-00; Thermo Fisher Scientific, Inc.). Lenti-X 293T cells were co-transfected with the lentiviral expression vectors pLenti-CMV-Puro-S1PR1 (custom lentiviral expression construct encoding human S1PR1) or pLentiCRISPR-v2 encoding OR51E1-targeting sgRNA or a non-targeting control, together with the packaging plasmids (pLP1, pLP2 and pVSVG), using Lipofectamine 2000 according to the manufacturer's instructions. Viral supernatants were collected 48 h post-transfection and filtered through a 0.45-μm membrane. Viral titers were determined using HT1080 cells, and LNCaP cells were transduced at a multiplicity of infection (MOI) of 5 in the presence of polybrene (8 μg/ml; MilliporeSigma). Transduced cells were selected with puromycin (1 μg/ml) for 7 days to establish pooled stable cell populations. OR51E1-knockout and non-targeting control LNCaP cells were generated by lentiviral transduction using lentiCRISPR constructs encoding sg*OR51E1* #1, sg*OR51E1* #2, or a non-targeting control sgRNA (sgCTL). The sgRNA target sequences were as follows: sg*OR51E1* #1: 5'-TAGCAG ACAAGCATCAAAC-3'; sg*OR51E1* #2: 5'-GGCCATAGA CGACATTGACC-3'; sgCTL: 5'-ACGGAGGCTAAGCGT CGCAA-3' (34). Following puromycin selection for 12 days, knockout efficiency was functionally validated by assessing NA-induced CRE-luciferase reporter activity. To assess the mutation of OR51E1 target, PCR was conducted using the primers 5'-CCTCCCTGGTTTAGAAGAGGC-3' and 5'-GGA TGCGCTGTCGAATCTCC-3'. The resulting PCR amplicon was digested with *BsrI* (New England BioLabs, Inc.) for

OR51E1 target #1 and *Hpa*II (Fermentas; Thermo Fisher Scientific, Inc.) for OR51E1 target #2 to confirm the knockout of OR51E1.

Reverse transcription-quantitative PCR (RT-qPCR). Total RNA was extracted and purified from cultured cells using the RNeasy Mini Kit (Qiagen, Inc.). First-strand cDNA was synthesized with the ReverTra Ace® RT-qPCR Kit (Toyobo Life Science) according to the manufacturer's instructions. Quantitative PCR was performed using the Brilliant SYBR Green QPCR Master Mix (Agilent Technologies, Inc.). The thermocycling conditions were as follows: Initial denaturation at 95˚C for 3 min, followed by 40 cycles of denaturation at 95˚C for 15 sec, annealing at 60˚C for 30 sec, and extension at 72˚C for 30 sec. Gene expression levels were normalized to the housekeeping gene β-actin, and relative quantification was performed using the $2^{-\Delta\Delta Cq}$ method (35). The primer sequences used for amplification were as follows: Actin forward, 5'-GGA AATCGTGCGTGACATTAAG-3' and reverse, 5'-AGCTCG TAGCTCTTCTCCA-3'; and OR51E1 forward, 5'-CCGCCA TTGGCCTGGACTCA-3' and reverse, 5'-CCAAGATGACGG GCAGCGGA-3'.

Cell proliferation assay. Cell proliferation was assessed using the Cell Counting Kit-8 (CCK-8; Dojindo Laboratories, Inc.). Cells were seeded in 96-well microplates at a density of 15,000 cells per well. For pathway inhibitor experiments, cells were pre-treated for 1 h with the indicated pathway inhibitors (SQ-22536, 100 μM (cat. no. 568500; MilliporeSigma; PubChem ID 5270); SU6656, 10 μM (cat. no. 572635; MilliporeSigma; PubChem ID 5312137); dasatinib, 10 nM (cat. no. CDS023389; MilliporeSigma; PubChem ID 3062316); SP600125, 10 μM (cat. no. HY-12041; MilliporeSigma; PubChem ID NSC75890); SB203580, 10 μM (cat. no. S1076; Selleck Chemicals; PubChem ID 176155); U0126, 1 μM (cat. no. HY-12031A; MilliporeSigma; PubChem ID 3006531); AG490, 10 μM (cat. no. HY-12000; MilliporeSigma; PubChem ID 5328779), followed by incubation with or without NA for 48 h. Subsequently, 10 μl of CCK-8 reagent was added to each well and incubated for 4 h at 37˚C. Absorbance was measured at 450 nm using an EnVision microplate reader (PerkinElmer, Inc.).

Apoptosis assay. LNCaP cells were plated in 12-well plates and treated with the indicated compounds for 24 h. After treatment, both the supernatant and adherent cells were collected using Accutase and resuspended in 100 μl of DPBS containing 0.1% BSA (cat. no. 11945; SERVA Electrophoresis GmbH) and annexin binding buffer (10 mM HEPES/NaOH, pH 7.4, 140 mM NaCl, 2.5 mM $CaCl_2$). Cells were stained with 10 μg/ml propidium iodide and 40 μl of Annexin V Ready Flow conjugates (Invitrogen; Thermo Fisher Scientific, Inc.) for 15 min at room temperature in the dark. Stained cells were analyzed by FACS Canto II (BD Biosciences), and data were processed using FlowJo software (version 10; BD Biosciences).

cAMP assay. Intracellular cAMP levels were measured using the pGloSensor-22F cAMP reporter plasmid (cat. no. E2301; Promega Corporation). Hana3A cells were plated in 24-well plates 24 h prior to transfection. One day before the assay, cells were transfected with plasmids encoding OR51E1 (20 ng), RTP1s (5 ng), the indicated GPCRs (5 ng), and the GloSensor-22F (50 ng) reporter using Lipofectamine 2000 (1 μl per well; Invitrogen; Thermo Fisher Scientific, Inc.), according to the manufacturer's instructions. The following day, cells were detached using DPBS containing EDTA and resuspended in CO_2-independent medium (Gibco; Thermo Fisher Scientific, Inc.) supplemented with 0.1% BSA and 800 μg/ml D-luciferin. Cells were transferred to white 96-well microplates (cat. no. 3917; Corning, Inc.) and incubated at room temperature for 2 h. Luminescence, reflecting intracellular cAMP levels, was measured using a TriStar2 microplate reader (Berthold Technologies GmbH) with a 540-nm filter.

CRE-luciferase reporter assay. LNCaP cells were seeded in 6-well cell culture plates at $4x10^5$ cells per well and transfected with the pGL4.29[luc2P/CRE/Hygro] reporter plasmid (400 ng; cat. no. E8471; Promega Corporation) using Lipofectamine 2000 (4 μl per well; Invitrogen; Thermo Fisher Scientific, Inc.), according to the manufacturer's instructions. After 48 h, cells were detached and replated into 96-well white plates. The following day, cells were starved with assay buffer (phenol red-free DMEM containing 0.1% BSA) overnight. After starvation, cells were treated with NA for 12 h at 37˚C. Luciferase activity was measured using the Steady-Glo® Luciferase Assay System (10 μl per well; Promega Corporation) for 5 min at room temperature in the dark using a TriStar2 LB 942 multimode microplate reader (Berthold Technologies GmbH).

Detection of cell surface expression of GPCRs. For ELISA, Hana3A cells were transfected with pcDNA-Lucy-FLAG-Rho-OR51E1 in 96 well plates. A total of 2 days after transfection, cells were fixed with 4% paraformaldehyde for 15 min at room temperature under non-permeabilizing conditions. Cells were incubated with anti-FLAG antibody (cat. no. F1804; MilliporeSigma; 1:4,000) at 4˚C overnight, followed by incubation with an HRP-conjugated anti-mouse antibody (cat. no. A9044; MilliporeSigma; 1:40,000) for 1 h in the dark. Cells were washed three times with PBS containing 1% BSA, incubated with TMB substrate (cat. no. 34028; Thermo Fisher Scientific, Inc.), and the reaction was stopped with sulfuric acid. Absorbance was measured at 450 nm using an EnVision Multilabel Plate Reader (Perkin Elmer, Inc.). For flow cytometry, LNCaP cells were dissociated using Accutase (cat. no. A6964; MilliporeSigma). Cells were incubated with an anti-S1PR1 rabbit polyclonal antibody (1:1,000) or control rabbit IgG (1:1,000) for 1 h at 4˚C, followed by incubation with a FITC-conjugated anti-rabbit IgG secondary antibody (1:1,000) for 30 min at 4˚C. Staining was performed in PBS containing 1% BSA. Cells were analyzed using a BD FACSCanto II cytometer equipped with a 488 nm laser and a 525/50 nm bandpass filter for FITC detection. At least 10,000 live events were collected per sample. Single cells were identified by forward scatter area (FSC-A) versus forward scatter height (FSC-H) gating, followed by exclusion of debris using FSC-A vs. side scatter area. Fluorescence-positive populations were gated based on unstained controls and fluorescence-minus-one controls for FITC. A viability dye was not used, and Fc-blocking was not applied because the cell lines used do not express Fc receptors under our culture conditions. Data were analyzed using FlowJo software.

Western blot analysis. Total protein was extracted using radioimmunoprecipitation assay lysis buffer (50 mM Tris-HCl, pH 7.4; 150 mM NaCl; 1% NP-40; 0.5% sodium deoxycholate; 0.1% SDS; 1 mM EDTA) supplemented with protease inhibitors (phenylmethyl sulfonyl fluoride, 10 mM; pepstatin, 1 mM; leupeptin, 1 mM; benzamide, 1 mM) and phosphatase inhibitors (sodium orthovanadate, 1 μM; β-glycerol phosphate, 10 mM; sodium pyrophosphate, 10 mM; sodium fluoride, 10 mM). Protein concentrations were determined using a Bio-Rad protein assay kit (Bio-Rad Laboratories Inc.). Equal amounts of proteins (25 μg per sample) were separated by SDS-PAGE using 10% acrylamide gels and transferred onto nitrocellulose membranes. Membranes were blocked with 5% non-fat milk in TBS containing 0.1% Tween-20 for 1 h and then incubated at 4˚C overnight with the following primary antibodies: anti-FLAG (1:4,000), phospho-Src (1:1,000), Src, phospho-SAPK/JNK (1:1,000), SAPK/JNK, phospho-p38 MAPK (1:1,000), p38 MAPK, phospho-ERK (1:1,000), ERK (1:1,000), PARP1 (1:2,000) and β-actin (1:20,000). Immunoreactive bands were detected using a chemiluminescent imaging system (AE-9150 Ez-Capture II; ATTO Corporation). Band intensities were quantified using ImageJ software (version 1.54p; National Institutes of Health).

Expression and survival analysis. Gene expression data for prostate adenocarcinoma (PRAD) and normal prostate tissue were obtained from the UCSC Xena Browser (https://xenabrowser.net/) using the dataset 'The Cancer Genome Atlas (TCGA) TARGET Genotype-Tissue Expression (GTEx) transcript expression by RSEM using UCSC TOIL RNA-seq recompute'. Transcript abundance was reported as RSEM transcripts per million (TPM). All TCGA and GTEx samples were processed through the UCSC TOIL RNA-seq recompute pipeline, which applies a uniform workflow for read alignment, quantification, normalization and quality control, thereby minimizing batch effects and enabling direct comparison of expression values between tumor and normal tissues. OR51E1 expression levels were compared between GTEx prostate samples and TCGA PRAD samples, including stratification by pathological stage where indicated. Expression levels were visualized using violin plots, and progression-free interval was assessed using Kaplan-Meier survival analysis. All analyses were performed using R software (version 4.1.2; R Foundation for Statistical Computing).

Statistical analysis. All experimental data are presented as the mean ± standard error of the mean (SEM). Statistical significance was determined using unpaired two-tailed Student's t-test, or two-way ANOVA followed by Tukey's multiple comparison test, as appropriate. $P<0.05$ was considered to indicate a statistically significant difference. Analyses were performed using GraphPad Prism 9 software (GraphPad Software; Dotmatics).

Results

OR51E1 suppresses PC cell proliferation, but its expression is not associated with patient survival. Among patients with cancer, OR51E1 expression is markedly higher in PRAD than in other cancer types (Fig. S1). To assess the effect of OR51E1 on PC cell survival, LNCaP cells were treated for 48 h with its saturated fatty acid ligands, NA and BA, and cell viability was measured. Consistent with previous studies (29,30), both NA and BA reduced LNCaP cell survival in a dose-dependent manner (Fig. 1A). To directly assess the role of OR51E1 in mediating NA-induced effects, OR51E1 knockout LNCaP cells were generated using CRISPR/Cas9-mediated gene editing. Successful knockout of OR51E1 was validated using restriction enzymes that target the PAM sites for sg*OR51E1* #1 and #2 (Fig. S2A and B). In addition, CRE-luciferase reporter assay showed a significant decrease in NA-induced reporter activity in OR51E1 knockout cells generated with two independent guide RNA (sg*OR51E1* #1 and #2), compared with control cells expressing a non-targeting sgRNA (sgCTL) (Fig. S2C). This confirms the effective ablation of NA-induced OR51E1 signaling. Notably, NA-induced reduction in cell viability observed in control LNCaP cells was completely abolished in OR51E1-knockout cells (Fig. 1B), demonstrating that NA-mediated growth inhibition is strictly dependent on OR51E1 expression. Consistent with this finding, NA-induced cytotoxicity was observed exclusively in LNCaP cells, which express OR51E1, but not in DU145 or PC3 cells, which lack OR51E1 expression (Fig. 1C and D). These results demonstrated that activation of OR51E1 by its agonist suppresses PC cell proliferation and that this anti-survival effect in PC cells is dependent on the presence of OR51E1.

Previous studies have reported that OR51E1 is significantly overexpressed in PC tissues compared with normal prostate tissues (28-30). To validate this observation, RNA-seq data from TCGA and the Genotype-Tissue Expression (GTEx) project were analyzed. The analysis confirmed a significant increase in OR51E1 mRNA expression in all stages of PC tissues relative to normal prostate tissues (Fig. 1E). However, OR51E1 expression levels revealed no significant association with overall survival (Fig. 1F), progression-free interval (Fig. 1G), disease-specific survival (Fig. S3A), or disease-free interval (Fig. S3B). These findings led us to hypothesize that although OR51E1 is an overexpressed anti-survival GPCR in PC, it may require interactions with other regulatory GPCRs to exert its tumor-suppressive effects. To test this possibility, a screening was performed to identify GPCRs that modulate OR51E1-mediated signaling.

S1PR1 enhances OR51E1-mediated cAMP signaling through increased surface expression. Previous studies have shown that class A GPCRs can interact with ectopically expressed ORs, suggesting a potential regulatory role in OR expression and signaling (23,36-39). To identify GPCRs that could potentially regulate OR51E1 signaling in PC, class A GPCRs were ranked based on their expression levels in the TCGA PRAD dataset. Receptors in the top quartile were then selected for functional screening, with the aim of prioritizing GPCRs that are robustly expressed in tumor tissues and more likely to act as physiologically relevant modulators of OR51E1 signaling (Fig. 2A). To evaluate their effects on OR51E1 signaling, Hana3A cells were co-transfected with OR51E1 and each selected GPCR, and then measured cAMP production upon stimulation with NA. Hana3A cells are a 293T-derived line that stably express RTP1, RTP2, REEP1 and Gαolf-accessory proteins that facilitate OR trafficking

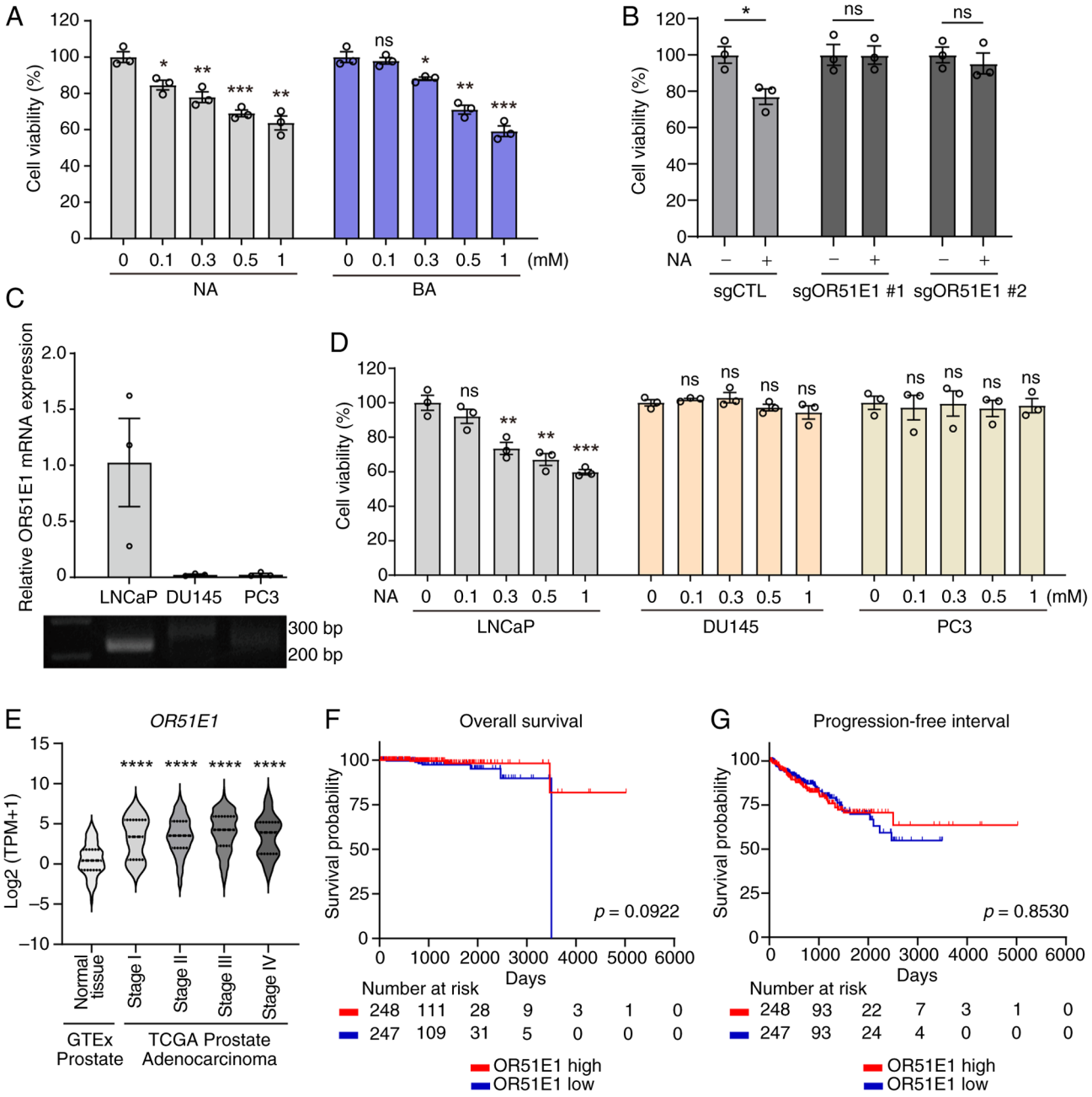

Figure 1. OR51E1 agonists reduce LNCaP cell viability, but expression alone does not predict patient outcome. (A) LNCaP cells were treated with increasing concentrations (0.1-1 mM) of NA or BA for 48 h, and cell viability was measured using the Cell Counting Kit-8 assay. Values were normalized to untreated controls. (B) The effect of NA on cell viability was assessed in control and OR51E1 knockout LNCaP cells after 48 h of NA (0.5 mM) treatment. (C) Relative OR51E1 mRNA expression in LNCaP, DU145, and PC3 prostate cancer cell lines was assessed by reverse transcription-quantitative PCR. Expression levels were normalized to β-actin. Representative PCR products were visualized by agarose gel electrophoresis. (D) LNCaP, DU145 and PC3 cells were cultured with various concentrations of NA for 48 h, and cell viability was measured. Data represent the mean ± SEM of three independent experiments. Statistical significance was determined using an unpaired Student's t-test. (E) OR51E1 expression across pathological stages of prostate cancer. OR51E1 mRNA expression levels were compared between normal prostate tissues from the GTEx dataset and prostate adenocarcinoma samples from TCGA stratified by pathological stage: Stage I (T2b), Stage II (T2b and T2c), Stage III (T3a and 3b), and Stage IV (T4). Transcript expression values (RSEM TPM) were obtained from the UCSC Xena Browser using the TCGA-TARGET-GTEx TOIL RNA-seq recompute dataset. Statistical significance was determined using an unpaired Student's t-test. (F and G) Kaplan-Meier survival curves for (F) overall survival and (G) progression-free interval stratified by OR51E1 expression levels. Red and blue lines indicate high- and low-expression groups, respectively. Survival probabilities were compared using the log-rank test, and P-values are shown in each panel. *P<0.05, **P<0.01, ***P<0.001 and ****P<0.0001. OR51E1, olfactory receptor 51E1; BA, butyric acid; NA, nonanoic acid; GTEx, Genotype-Tissue Expression; TCGA, The Cancer Genome Atlas; ns, not significant.

and function, and are widely used for heterologous OR expression studies (36-39).

Among the GPCRs tested, LPAR2, EDNRA, S1PR1, ATGR1, LPAR1 and GPR146 significantly enhanced NA-induced cAMP production, whereas GPR176 and FFAR2 suppressed it (Fig. 2B). Notably, S1PR1 produced the strongest enhancement despite being a Gαi-coupled receptor, which typically does not directly increase cAMP levels, highlighting it as a key candidate for further study. Co-expression of OR51E1 with increasing amounts of S1PR1 plasmid DNA

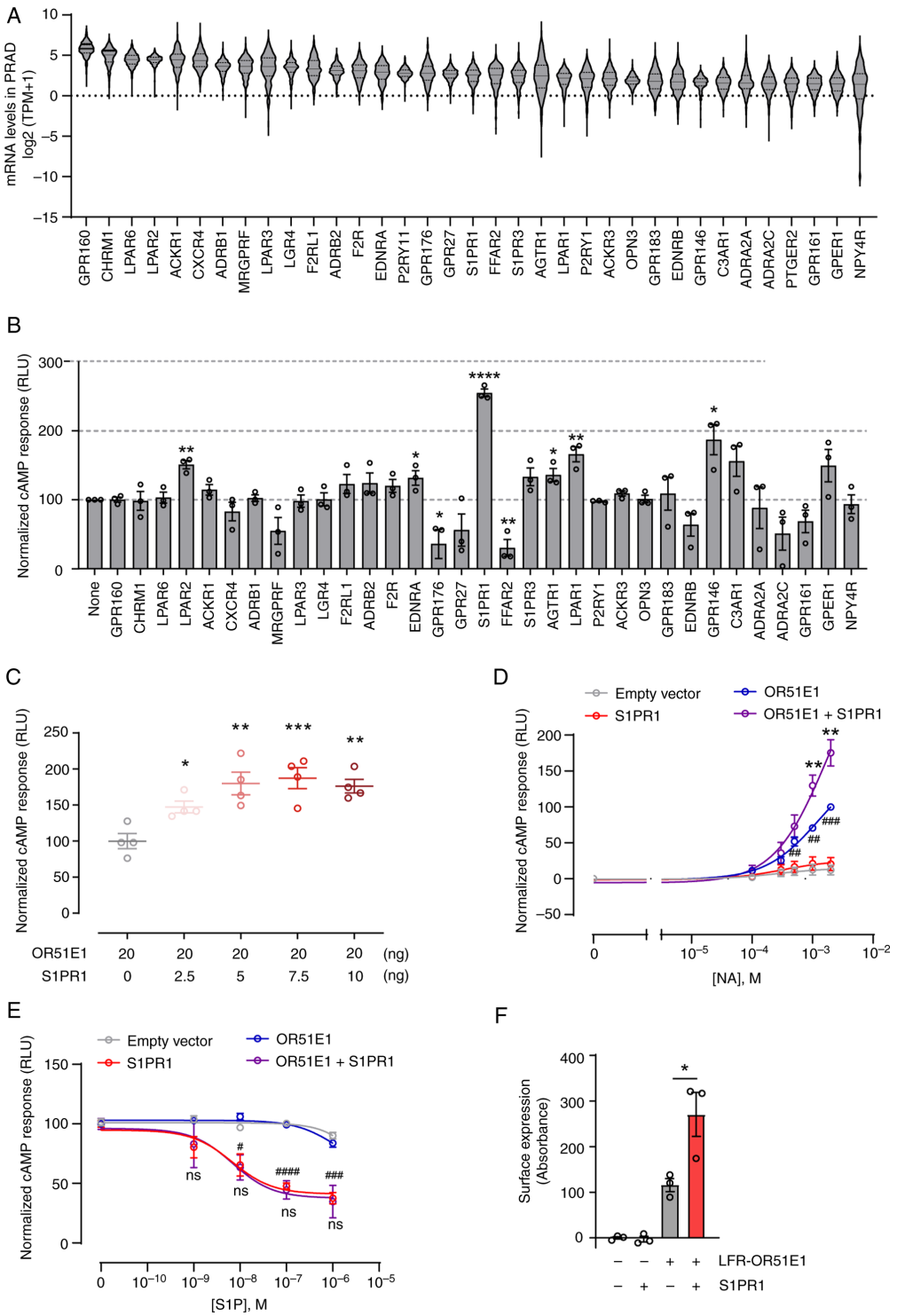

Figure 2. Identification of S1PR1 as a GPCR enhancer of OR51E1 signaling. (A) Class A GPCRs with the highest quartile of mRNA expression in The Cancer Genome Atlas PRAD. Violin plots show median TPM values for each GPCR. (B) Hana 3A cells were transfected with Rho-Flag-OR51E1 alone or co-transfected with individual candidate GPCRs from (A) NA (1 mM)-induced cAMP production was measured using the Glosensor-22F cAMP reporter assay and normalized to OR51E1-only controls. Data were analyzed by an unpaired Student's t-test. (C) Dose-dependent effect of S1PR1 on OR51E1 signaling. Hana3A cells were transfected with a constant amount of OR51E1 plasmid (20 ng) and increasing amounts of S1PR1 plasmid (0-10 ng). cAMP production was analyzed using an unpaired Student's t-test. (D) Hana3A cells were transfected with empty vector, OR51E1, S1PR1, or OR51E1 together with S1PR1 along with the GloSensor-22F cAMP reporter. Cells were stimulated with increasing concentrations of NA (0.1-2 mM), and cAMP production was measured. Statistical significance was determined using an unpaired Student's t-test. Asterisks (*) indicate significance differences between OR51E1 and OR51E1 + S1PR1 groups, and hash symbols (#) indicate significance differences between empty vector and OR51E1 groups. (E) Hana3A cells were transfected as described in (D) and treated with increasing concentrations of S1P (1-1,000 nM) in the presence of forskolin (1 μM). Statistical significance was determined using an unpaired Student's t-test. Asterisks (*) indicate significance differences between S1PR1 and OR51E1 + S1PR1 groups, and hash symbols (#) indicate significance differences between empty vector and S1PR1 groups. (F) Surface expression of Lucy-Rho-FLAG (LFR)-tagged OR51E1 was measured by ELISA under non-permeabilized conditions in the presence or absence of co-transfected S1PR1. Surface expression was calculated by subtracting optical density values from vector-only controls. Data represent the mean ± SEM of three independent experiments and were analyzed using an unpaired Student's t-test. *P<0.05, **P<0.01, ***P<0.001 and ****P<0.0001; $^{\#}$P<0.05, $^{\#\#}$P<0.01, $^{\#\#\#}$P<0.001 and $^{\#\#\#\#}$P<0.0001. S1PR1, sphingosine-1-phosphate receptor 1; GPCR, G-protein-coupled receptor; PRAD, prostate adenocarcinoma; TPM, transcripts per million; ns, not significant.

led to a dose-dependent enhancement of NA-induced cAMP signaling (Fig. 2C). By contrast, co-expression of OR51E1 with dopamine receptor D2 (DRD2), another Gαi-coupled receptor, failed to augment NA-induced cAMP production (Fig. S4), confirming that the effect is specific to S1PR1 rather than a general property of Gαi-coupled GPCRs.

NA did not induce cAMP responses in cells transfected with an empty vector, whereas robust cAMP production was observed in cells overexpressing OR51E1 (Fig. 2D), indicating that NA-induced cAMP signaling is specifically mediated by OR51E1. OR51E1-mediated cAMP responses increased in a dose-dependent manner at higher NA concentrations (1-2 mM) and were further enhanced by S1PR1 co-expression (Fig. 2D). To assess potential reciprocal regulation, S1PR1 signaling was examined in the presence of OR51E1. In S1PR1-expressing cells, forskolin-induced cAMP production was suppressed by S1P, and co-expression of OR51E1 did not alter this suppression (Fig. 2E), indicating that OR51E1 does not modulate S1PR1 signaling. Finally, to investigate the mechanism by which S1PR1 enhances OR51E1 signaling, OR51E1 surface expression under non-permeabilized conditions was measured using an ELISA. OR51E1 was tagged with a Lucy-Flag-Rho sequence, which promotes OR surface trafficking (32,40,41). Co-expression of S1PR1 significantly increased the surface localization of OR51E1 (Fig. 2F). By contrast, OR51E1 mRNA levels were unaffected by S1PR1 co-expression (Fig. S5), suggesting that S1PR1 enhances OR51E1 function primarily by facilitating post-transcriptional trafficking to the plasma membrane rather than by transcriptional upregulation in Hana3A cells.

S1PR1 expression enhances OR51E1-mediated inhibition of PC cell survival. To examine the role of S1PR1 in OR51E1-mediated inhibition of PC cell survival, LNCaP cells, which lack detectable S1PR1 expression (Fig. S6A), were transfected with an S1PR1 expression construct. NA-induced inhibition of cell survival was significantly enhanced in S1PR1-transfected LNCaP cells, but not in cells transfected with DRD2 (Fig. 3A). Similarly, BA enhanced OR51E1-mediated inhibition of LNCaP survival only in the presence of S1PR1 (Fig. S7). To further clarify the mechanism, a stable LNCaP cell line overexpressing S1PR1 (LNCaP-S1PR1) was generated via lentiviral transduction. Flow cytometric analysis confirmed robust surface expression of S1PR1 in these cells (Fig. S6B). NA treatment led to a dose-dependent decrease in cell survival, with a more pronounced effect in LNCaP-S1PR1 cells compared with parental cells (Fig. 3B). These findings suggested that S1PR1 expression enhances the anti-survival effect of OR51E1 activation in PC cells. To determine whether reduced cell survival was attributable to apoptosis, Annexin-V/PI staining was performed. NA treatment induced both early and late apoptosis in a dose-dependent manner, and this effect was significantly amplified in LNCaP-S1PR1 cells (Figs. 3C and S8). Consistently, NA treatment increased caspase-3 activation and PARP1 cleavage, with more pronounced effects observed in the presence of S1PR1 (Fig. 3D and E).

To assess whether S1PR1 activation further modulates OR51E1 function, the effect of NA on apoptosis was examined in the presence or absence of TC-G1006, a selective S1PR1 agonist. TC-G1006 significantly potentiated NA-induced apoptosis only in S1PR1-overexpressing cells, indicating that ligand-induced S1PR1 activation enhances OR51E1-mediated apoptosis (Figs. 4A and S9A-C). Notably, TC-G1006 alone did not induce apoptosis in either parental or S1PR1-expressing cells, suggesting that S1PR1 activation alone is insufficient to trigger PC cell apoptosis but can potentiate the effect of NA. In LNCaP-S1PR1 cells, TC-G1006 also potentiated NA-induced growth inhibition, and this effect was abolished by co-treatment with either pertussis toxin or NIBR-0213, a selective antagonist of S1PR1 (Fig. 4B), confirming that the enhancement requires ligand-induced S1PR1 activation. However, neither pertussis toxin nor NIBR-0213 reversed NA-induced growth inhibition in LNCap-S1PR1 cells, indicating that S1PR1 augments OR51E1 function not only through agonist-induced activation but also via its basal activity, independent of Gi signaling. Taken together, these findings demonstrate that both S1PR1 expression and activation enhance OR51E1-mediated proliferation inhibition and apoptosis in PC cells.

Co-expression of OR51E1 and S1PR1 correlates with improved prognosis in patients with PC. To assess the clinical relevance of S1PR1 and OR51E1 in PC, RNA-seq data from the TCGA PRAD cohort were analyzed. Patients were stratified into four groups based on OR51E1 and S1PR1 mRNA expression levels: High expression of both (OHSH), high OR51E1 and low S1PR1 (OHSL), low OR51E1 and high S1PR1 (OLSH), and low expression of both (OLSL). Progression-free interval differed significantly among the four groups, with the OHSH group showing the highest survival probability and the OLSL group the lowest (Fig. 5A). When patients were divided into the 'both high (OHSH)' group versus all other groups combined, the OHSH group again exhibited significantly improved progression-free interval (Fig. 5B). Stage-stratified analyses revealed that high OR51E1-S1PR1 co-expression was significantly associated with improved progression-free interval in stage II patients (Fig. 5C), while a similar trend was observed in stage III patients but did not reach statistical significance (Fig. 5D). Analyses of stage I and IV patients were limited by small sample sizes, precluding definitive conclusions (Fig. S10). Collectively, these results suggested that co-expression of OR51E1 and S1PR1 is associated with improved prognosis in PC regardless of tumor stages.

These clinical observations are consistent with the experimental findings that OR51E1 suppresses PC cell survival and that S1PR1 enhances OR51E1-mediated apoptosis. Collectively, these results suggested that S1PR1 co-expression potentiates the tumor-suppressive function of OR51E1 and contributes to improved clinical outcomes in PC. Targeting this axis may represent a novel therapeutic strategy to limit disease progression.

S1PR1 enhances OR51E1-mediated Src-JNK signaling to inhibit PC cell survival. To investigate the downstream signaling pathways involved in NA-induced cell death in PC, LNCaP cells were pretreated with pharmacological inhibitors targeting key nodes of the canonical Gs/olf-cAMP pathway and alternative signaling pathways. Inhibition of adenylate cyclase with SQ22536, which blocks canonical Gs/olf-mediated cAMP production, failed to rescue NA-induced

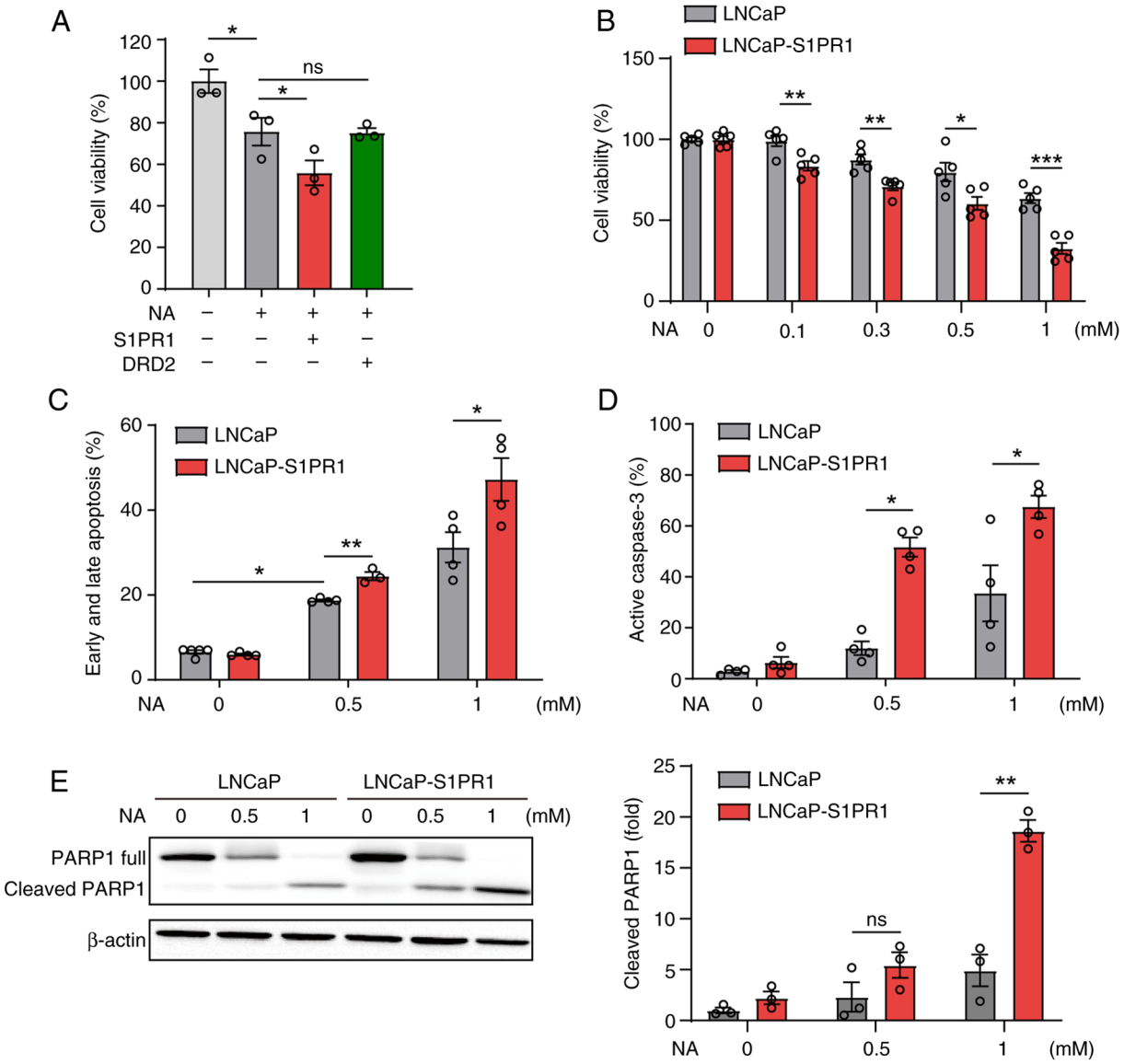

Figure 3. S1PR1 enhances OR51E1-mediated cytotoxicity and apoptosis in LNCaP cells. (A) LNCaP cells were transfected with an empty vector, S1PR1, or DRD2. After 48 h, cells were treated with NA (0.5 mM) for an additional 48 h, and cell viability was measured using the Cell Counting Kit-8 assay. (B) LNCaP cells were transduced with lentivirus encoding S1PR1 and selected with puromycin (1 μg/ml). Cell viability of parental LNCaP and LNCaP-S1PR1 cells was measured 48 h after treatment with increasing concentrations of NA (0.1-1 mM). (C) Apoptosis was assessed in LNCaP cells treated with NA for 48 h using annexin V/PI staining. Apoptotic cells were quantified as the percentage of annexin V-positive cells (early apoptosis) and annexin V/PI double-positive cells (late apoptosis) relative to the total cell population. (D) Caspase-3 activation was measured by flow cytometry following NA treatment. (E) PARP1 cleavage was analyzed by western blotting in NA-treated cells. Band intensities were quantified using ImageJ software. Data represent the mean ± SEM of at least three independent experiments. Statistical significance was determined using an unpaired Student's t-test. *P<0.05, **P<0.01 and ***P<0.001. S1PR1, sphingosine-1-phosphate receptor 1; OR51E1, olfactory receptor 51E1; DRD2, dopamine receptor D2; NA, nonanoic acid; PI, propidium iodide; ns, not significant.

inhibition of proliferation (Fig. 6A). Similarly, inhibition of PKA with H-89 and inhibition of the exchange protein directly activated by cAMP (EPAC) with ESI-09 did not attenuate NA-induced suppression of proliferation. By contrast, inhibition of Src kinase with SU6656 significantly but only partially restored cell viability in NA-treated cells. These results indicated that canonical Gs/olf-cAMP signaling is dispensable for OR51E1-mediated anti-survival effects and instead support the involvement of an alternative Src-dependent signaling pathway in NA-induced PC cell death.

To further delineate the underlying mechanisms, activation of key signaling pathways including Src, JNK, p38 MAPK and ERK, was examined following NA treatment. Immunoblotting revealed a rapid increase in Src phosphorylation, peaking at 15 min (Fig. S11A and B), and a gradual increase in JNK phosphorylation up to 1 h (Fig. S11C). Phosphorylation of p38 MAPK was also detected as early as 5 min after NA treatment (Fig. S11D), whereas ERK phosphorylation remained unchanged (Fig. S11E).

To determine which pathway contributes to NA-induced inhibition of proliferation, cells were treated with NA in the presence of specific inhibitors: SU6656 and Dasatinib (Src inhibitors), SP600125 (JNK inhibitor), U0126 (MEK/ERK inhibitor), SB203580 (p38 inhibitor) and AG490 (JAK/STAT3 inhibitor). NA-induced cell death was attenuated by SU6656, dasatinib and SP600125, but not by SB203580, U0126, or

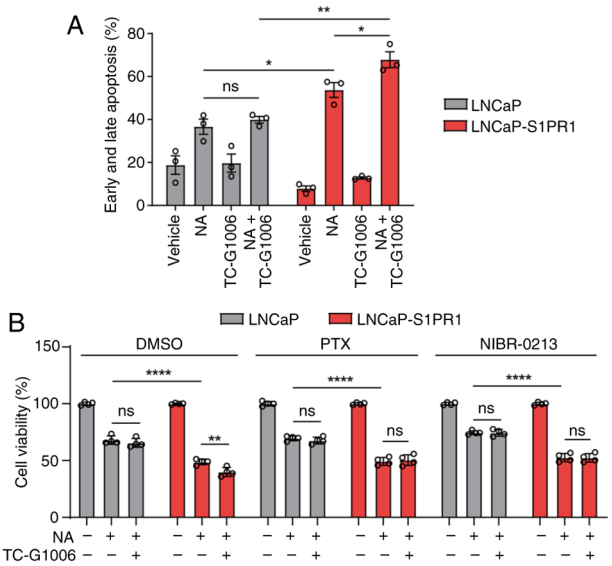

Figure 4. Activation of S1PR1 enhances OR51E1-mediated apoptosis in LNCaP cells. (A) LNCaP and LNCaP-S1PR1 cells were treated with NA, TC-G1006 (a selective S1PR1 agonist), or both for 48 h, and apoptosis was assessed using annexin V/PI staining. (B) LNCaP and LNCaP-S1PR1 cells were preincubated with DMSO, PTX, or NIBR-0213 (a selective S1PR1 antagonist) for 1 h and then treated with NA for 48 h. Cell viability was measured using the CCK-8 assay. Data represent the mean ± SEM of at least three independent experiments. Statistical analysis was performed using two-way ANOVA with Tukey's multiple comparison test. *P<0.05, **P<0.01 and ****P<0.0001. S1PR1, sphingosine-1-phosphate receptor 1; OR51E1, olfactory receptor 51E1; NA, nonanoic acid; PI, propidium iodide; DMSO, dimethyl sulfoxide; PTX, pertussis toxin; ns, not significant.

AG490 (Fig. 6B), indicating that Src and JNK, but not p38, ERK, or STAT3, play a role in NA-mediated inhibition of proliferation. Although NA robustly activated p38, its inhibition did not affect cell viability, suggesting that p38 is dispensable in this context.

Consistent with the enhanced apoptosis observed in S1PR1-overexpressing LNCaP cells, NA-induced JNK phosphorylation was more pronounced in LNCaP-S1PR1 cells than in parental cells (Fig. 6C). Moreover, SU6656 treatment reduced NA-induced JNK phosphorylation (Fig. 6D), indicating that JNK activation occurs downstream of Src signaling. Both SU6656 and dasatinib partially restored cell viability and suppressed NA-induced apoptosis in LNCaP cells regardless of S1PR1 expression (Fig. 6E and F; Fig. S12A-C), confirming the critical role of the Src-JNK axis in mediating NA-induced apoptosis. Taken together, these findings demonstrated that NA-induced inhibition of proliferation in PC cells is mediated primarily through Src activation followed by JNK phosphorylation, rather than through classical G protein-cAMP signaling.

Discussion

Previous studies have reported that certain ORs overexpressed in cancer can exert either pro-tumorigenic or anti-tumorigenic effects (42-45). However, a clear relationship between OR overexpression and patient survival has rarely been established. OR51E1 is highly expressed in PC cells and has been identified to inhibit cancer cell proliferation (29,30). Consistent with these findings, it was confirmed that NA- or BA-induced reduction in cell survival occurred specifically in LNCaP cells, which endogenously express OR51E1 (Fig. 1A). Importantly, this anti-survival effect was abrogated in OR51E1-knockout LNCaP cells, demonstrating that NA-mediated suppression of proliferation is dependent on the presence of OR51E1 (Fig. 1B). By contrast, NA-induced cytotoxicity was not observed in DU145 or PC3 PC cell lines, which lack OR51E1 expression (Fig. 1C and D). Although ectopic overexpression of OR51E1 in these cell lines would provide a direct test of whether OR51E1-mediated anti-survival effects are broadly conserved across PC models, such experiments were beyond the scope of the present study. Nevertheless, the current data provide strong evidence that OR51E1 is required for NA-induced suppression of proliferation in PC cells that express this receptor.

In the present analysis of the TCGA dataset, OR51E1 was significantly overexpressed across all stages of prostate carcinoma compared with normal prostate tissue; however, its expression level was not significantly associated with patient survival (Fig. 1F and G). Based on these findings, it was hypothesized that the tumor-suppressive function of OR51E1-potentially shared by other ORs-may be regulated by additional GPCRs. To identify GPCRs that modulate OR51E1 function in PC cells, the expression profiles of class A GPCRs were first examined in PC tissues (Fig. 2A) and the effects of highly expressed GPCRs on NA-induced OR51E1 activation were subsequently evaluated in Hana3A cells (Fig. 2B). Through this screening approach, S1PR1 was identified as a candidate GPCR that enhances OR51E1 function by amplifying OR51E1-mediated cAMP signaling (Fig. 2B-D). Expression of S1PR1 in LNCaP cells, which endogenously express OR51E1, significantly increased NA-induced inhibition of proliferation and apoptosis (Fig. 3). Furthermore, activation of S1PR1 with its selective agonist TC-G1006 further potentiated OR51E1-mediated inhibition of proliferation (Fig. 4). Importantly, analysis of TCGA patient dataset revealed that high expression of both OR51E1 and S1PR1 was associated with significantly improved progression-free interval, whereas OR51E1 expression alone had no prognostic value (Fig. 1E and F; Fig. 5). Collectively, these findings suggested that S1PR1 enhances the tumor-suppressive function of OR51E1 and may contribute to improved clinical outcomes in PC.

Mechanistically, it was found that NA-induced, OR51E1-mediated inhibition of proliferation in LNCaP cells was dependent on the Src-JNK axis rather than the canonical Gs/olf-cAMP pathway (Fig. 6). Inhibitors of Src and JNK abrogated both NA-induced apoptosis and the enhancing effects of S1PR1, suggesting that S1PR1 promotes OR51E1 function through a shared signaling pathway. Importantly, inhibition of Src or JNK only partially attenuated NA-induced inhibition of proliferation and apoptosis, indicating that although the Src-JNK axis represents a major downstream pathway of OR51E1 activation, additional signaling mechanisms are likely to contribute to the full anti-survival response. While it remains unclear whether Src-JNK signaling directly induces apoptosis or indirectly facilitates OR51E1 function by increasing trafficking or membrane localization, the current data support both possibilities. In Hana3A cells, co-expression of S1PR1 significantly increased the surface expression of OR51E1 without affecting OR51E1 mRNA levels (Figs. 2G and S3), indicating a

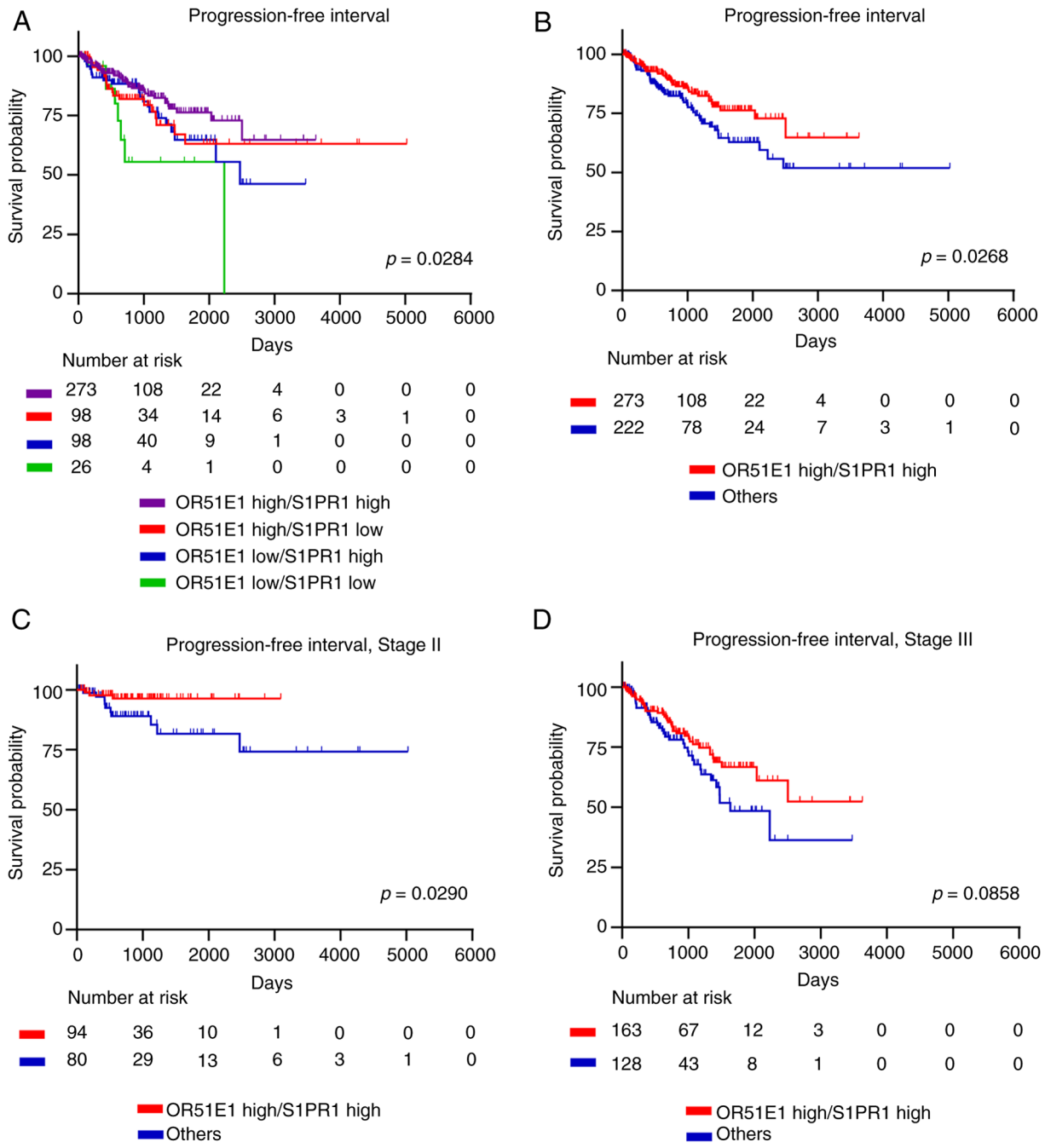

Figure 5. Co-expression of OR51E1 and S1PR1 correlates with improved progression-free interval in patients with prostate cancer. (A) Kaplan-Meier analysis of progression-free interval in patients with PRAD from TCGA. Patients were stratified into four groups based on the expression levels of OR51E1 and S1PR1: high expression of both genes, high OR51E1 and low S1PR1, low OR51E1 and high S1PR1, and low expression of both genes. (B) Kaplan-Meier analysis of progression-free interval in patients with PRAD stratified into two groups: High expression of both OR51E1 and S1PR1 versus all other groups combined. (C) Stage II-specific Kaplan-Meier analysis of progression-free interval stratified by OR51E1 and S1PR1 co-expression status. (D) Stage III-specific Kaplan-Meier analysis of progression-free interval stratified by OR51E1 and S1PR1 co-expression status. Survival differences were assessed using the log-rank test, and pooled log-rank P-values are shown in each panel. OR51E1, olfactory receptor 51E1; S1PR1, sphingosine-1-phosphate receptor 1; PRAD, prostate adenocarcinoma.

post-transcriptional regulatory mechanism. Unfortunately, due to the lack of suitable antibodies, it was not possible to detect endogenous OR51E1 surface expression in LNCaP cells.

Although NA-induced cytotoxicity is mediated by Src-JNK signaling, OR51E1-driven cAMP signaling remains a robust and reproducible response in both Hana3A cells and LNCaP cells endogenously expressing OR51E1. However, pharmacological inhibition of adenylyl cyclase, PKA, or EPAC did not attenuate NA-induced inhibition of proliferation or apoptosis, indicating that canonical Gs/olf-cAMP signaling is dispensable for the anti-survival effects of OR51E1 activation. These findings suggested that OR51E1 engages parallel signaling pathways in PC cells, with non-canonical Src-JNK signaling mediating cytotoxicity, while the functional role of cAMP signaling may be context-dependent and warrants further investigation.

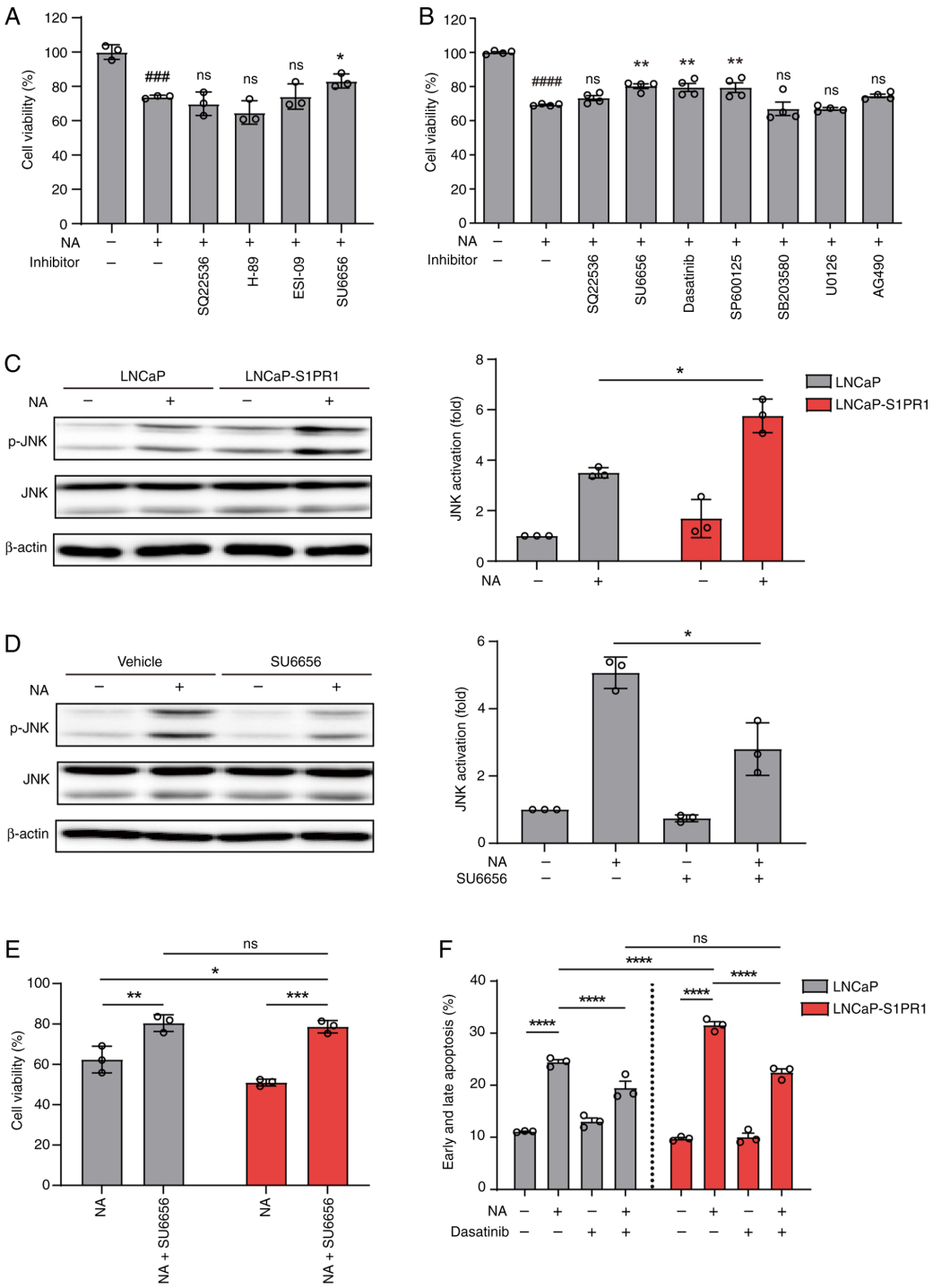

Figure 6. Co-expression of S1PR1 amplifies OR51E1-Src-JNK signaling and suppression of proliferation. (A and B) Inhibitor profiling reveals signaling pathways involved in NA-induced reduction of LNCaP cell viability. LNCaP cells were preincubated for 1 h with (A) canonical OR pathway inhibitors (SQ-22536, 100 μM; H-89, 3 μM; ESI-09, 3 μM; SU6656, 10 μM) or with (B) other, less well-characterized pathway inhibitors (SU6656, 10 μM; Dasatinib, 10 nM; SP600125, 3 μM; SB203580, 3 μM; U0126, 10 μM; AG-490, 10 μM), followed by treatment with NA for 48 h. SQ-22536 and SU6656 were included in both panels for comparison. Cell viability was measured using the CCK-8 assay. Data represent the mean ± SEM of at least three independent experiments. Statistical analysis was performed using an unpaired Student's t-test. Hash symbols (#) indicate statistical significance between vehicle- and NA-treated cells, whereas asterisks (*) indicate statistical significance between cells treated with NA alone and those co-treated with NA and the indicated inhibitors. (C) Western blot analysis of JNK activation in LNCaP and LNCaP-S1PR1 cells treated with NA for 1 h. Protein levels of p-JNK and total JNK were analyzed. (D) Effect of Src inhibition on NA-induced JNK activation. LNCaP cells were pretreated with the Src inhibitor SU6656 (10 μM) for 1 h and then treated with NA for 1 h. Protein levels of p-JNK and total JNK were assessed. Band intensities were quantified using ImageJ software. Data represent the mean ± SEM of three independent experiments. Statistical significance was determined using an unpaired Student's t-test. (E) Effect of Src inhibition on NA-mediated suppression of proliferation. LNCaP and LNCaP-S1PR1 cells were pretreated with SU6656 for 1 h, and cell viability was measured using the CCK-8 assay after NA treatment. Data represent the mean ± SEM of at least three independent experiments and were analyzed using two-way ANOVA with Tukey's multiple comparison test. (F) Effect of Src inhibition on NA-induced apoptosis. LNCaP and LNCaP-S1PR1 cells were pretreated with dasatinib (100 nM) for 1 h and then treated with NA. Apoptosis was assessed using annexin V/PI staining. Data represent the mean ± SEM of three independent experiments and were analyzed using two-way ANOVA with Tukey's multiple comparison test. $^{###}$P<0.001 and $^{####}$P<0.0001; *P<0.05, **P<0.01, ***P<0.001 and ****P<0.0001. S1PR1, sphingosine-1-phosphate receptor 1; OR51E1, olfactory receptor 51E1; NA, nonanoic acid; CCK-8, Cell Counting Kit-8; p-, phosphorylated; PI, propidium iodide; ns, not significant.

In Hana3A cells, expression of S1PR1 enhanced NA-induced cAMP responses when co-expressed with OR51E1 (Fig. 2C and D), despite S1PR1 being a Gαi-coupled receptor that does not independently stimulate cAMP production. In LNCaP cells, overexpression of S1PR1 alone did not produce a statistically significant increase in apoptosis (Fig. 3C-E). These findings suggested that S1PR1 by itself is insufficient to induce apoptosis but can amplify NA-induced OR51E1-dependent anti-survival effects. Because the apoptosis-inducing effect of NA is independent of the canonical Gs/olf-cAMP pathway, and Src and JNK activation was not directly examined in Hana3A cells co-expressing OR51E1 and S1PR1, it remains unclear whether S1PR1 expression alone, in the absence of OR51E1, can activate the Src/JNK pathway in this heterologous system.

Several studies have demonstrated that class A GPCRs can form heteromers with ORs both *in vitro* and *in vivo* (23,36-39). For example, the β_2-adrenergic receptor, purinergic receptors (P2Y1 and P2Y2), and the adenosine 2A receptor promote both ERK activation and surface expression of OR-M71 through heteromerization (36,37). Similarly, the muscarinic acetylcholine receptor 3 forms heteromers with OR-S6, enhancing OR signaling via a β-arrestin-dependent mechanism without altering surface localization (38,39). While S1PR1 has been reported to interact with other GPCRs (46,47), the observed enhancement of OR51E1 signaling could arise from multiple mechanisms, including receptor heteromerization or indirect effects on receptor trafficking. At present, there is no direct evidence for a physical interaction or signaling crosstalk between OR51E1 and S1PR1, and both possibilities therefore remain speculative.

An alternative hypothesis for the enhancement of OR51E1's tumor-suppressive function by S1PR1 is that S1PR1 influences OR51E1 localization and activity through signaling crosstalk. Previous studies have revealed that S1PR1 activation regulates various vesicular trafficking systems, including internal vesicles in hippocampal neurons (46), exosomal multivesicular bodies (47), and transport carriers in the trans-Golgi network (48). These findings suggest that S1PR1 may regulate the intracellular trafficking and membrane localization of OR51E1 in PC cells.

The JNK pathway is known to promote apoptosis and inhibit proliferation in PC (49-52). For example, mitogen-activated kinase phosphatase 1, which is upregulated by oncogenes, suppresses apoptosis by inhibiting JNK activity in PC (53). In the present study, inhibition of JNK attenuated NA-induced inhibition of proliferation, supporting its role in mediating OR51E1-induced apoptosis. This finding is consistent with previous findings showing that JNK phosphorylation is absent in well-, moderately-, and poorly differentiated tumors in the transgenic adenocarcinoma mouse prostate model, despite activation of ERK and p38 in well-differentiated tumors (54).

Moreover, studies on OR51E1 and OR51E2 in PC cells have demonstrated their tumor-suppressive activity through Src kinase-dependent, rather than G-protein-mediated, signaling (29,30,55). The findings of the present study align with this model: Adenylyl cyclase inhibition did not affect OR51E1 function, whereas NA stimulation induced rapid Src phosphorylation within 5 min. Inhibition of Src not only blocked JNK activation but also restored cell viability and suppressed NA-induced apoptosis. These results indicated that OR51E1 mediates tumor suppression in PC via a Src-JNK-dependent pathway.

In addition to these mechanistic insights, emerging evidence suggests that the metabolite-sensing functions of ORs may link tumor metabolism to signaling outcomes. ORs are increasingly recognized as metabolite-sensing GPCRs that can link cellular metabolism to signaling outcomes. In PC, metabolic reprogramming, particularly involving lipid and short-chain fatty acid metabolism, plays a critical role in disease progression and therapy resistance. Notably, acetate utilization has been shown to promote hormone therapy resistance through metabolic reprogramming and neuroendocrine differentiation, highlighting the pathological relevance of short-chain fatty acids in PC progression (56). Furthermore, metabolic inputs, such as pyruvate flux through the mitochondrial pyruvate carrier, can influence cell fate decisions and antitumor function in immune cells, underscoring the broader principle that metabolic signals can regulate cellular behavior (57). Collectively, these findings suggest that OR51E1, as a fatty acid-sensing receptor, may function as a metabolic sensor that links changes in tumor metabolite availability to non-canonical signaling pathways, including Src-JNK activation, thereby influencing PC cell survival and progression.

The present study demonstrates the involvement of the OR51E1 signaling axis in PC using LNCaP cells as an *in vitro* model. Importantly, transcriptomic analyses of TCGA and GTEx datasets revealed that OR51E1 is not only highly expressed in PRAD but also shows significantly elevated expression in other cancer types such as kidney renal clear cell carcinoma (KIRC) and glioblastoma multiforme (GBM) compared with corresponding normal tissues. These observations suggest that OR51E1's ectopic expression and potential functional roles may extend beyond PC. Supporting this notion, previous studies have reported OR51E1 expression in neuroendocrine tumors of the small intestine and lung carcinoid tumors, where it may serve as a biomarker and contribute to tumor biology (25,27). Furthermore, recent single-cell transcriptomic analyses in GBM have indicated cell type-specific expression of OR51E1 within the tumor microenvironment, implicating it in processes such as vascular remodeling and tumor progression (58). Overall, these observations raise the possibility that the OR51E1 signaling axis characterized in LNCaP cells may also play a role in other OR51E1-expressing cancers such as KIRC and GBM. However, given that the current functional analyses were limited to a single cell line, further investigations using additional *in vitro* and *in vivo* models are necessary to confirm the broader relevance and mechanistic involvement of OR51E1 in diverse tumor types.

A limitation of the present study is the absence of rescue experiments in which an sgRNA-resistant OR51E1 is re-expressed in OR51E1-knockout cells. Such experiments would further strengthen the causal link between OR51E1 and NA-induced Src/JNK activation and apoptosis and will be addressed in future studies. It is also acknowledged that the survival analyses were stratified only by pathological stage and did not account for other clinical covariates, such as

Gleason score, PSA at diagnosis, or patient age. Future studies using larger and more comprehensively annotated clinical cohorts will be required to determine whether OR51E1-S1PR1 co-expression is independently associated with prognosis after multivariate adjustment for these factors.

In conclusion, the current findings reveal that although OR51E1 is overexpressed in PC and exerts anti-tumorigenic effects, its impact on patient prognosis is not apparent when considered in isolation. However, the identification of S1PR1 as a co-regulator that enhances OR51E1-mediated signaling and apoptosis provides new insight into the contextual regulation of ORs in cancer. The observed synergy between OR51E1 and S1PR1, both *in vitro* and in patient datasets, suggests that the tumor-suppressive activity of OR51E1 may depend on co-expression with specific GPCR partners. These results highlight the importance of receptor interactions and signaling context in evaluating the functional and clinical relevance of ectopically expressed ORs in cancer. Targeting such receptor networks may offer novel therapeutic strategies for PC and other malignancies in which ORs are dysregulated.

Acknowledgements

The authors would like to thank Dr Jae-Yeon Jeong (GPCR Therapeutics Inc.) for helpful comments and discussions.

Funding

The present study was supported by the National Research Foundation of Korea (grant nos. RS-2020-NR049538 and 2021R1A2C1013718) and Samsung Science and Technology Foundation (grant no. SSTF-BA1901-09).

Availability of data and materials

The data generated in the present study may be requested from the corresponding author.

Authors' contributions

KK, JL, CC, JB, HJC and WKH conceived and designed experiments. KK performed experiments. KK and WKH analyzed data and wrote the manuscript. All authors reviewed and commented on the manuscript. All authors read and approved the final version of the manuscript. KK and WKH confirm the authenticity of all the raw data.

Ethics approval and consent to participate

Not applicable.

Patient consent for publication

Not applicable.

Competing interests

WKH is a shareholder in GPCR Therapeutics Inc. The other authors declare that they have no competing interests.

Use of artificial intelligence tools

During the preparation of this work, artificial intelligence tools were used to improve the readability and language of the manuscript or to generate images, and subsequently, the authors revised and edited the content produced by the artificial intelligence tools as necessary, taking full responsibility for the ultimate content of the present manuscript.

References

1. Bjarnadóttir TK, Gloriam DE, Hellstrand SH, Kristiansson H, Fredriksson R and Schiöth HB: Comprehensive repertoire and phylogenetic analysis of the G protein-coupled receptors in human and mouse. Genomics 88: 263-273, 2006.
2. Godfrey PA, Malnic B and Buck LB: The mouse olfactory receptor gene family. Proc Natl Acad Sci USA 101: 2156-2161, 2004.
3. Malnic B, Godfrey PA and Buck LB: The human olfactory receptor gene family. Proc Natl Acad Sci USA 101: 2584-2589, 2004.
4. Boekhoff I, Tareilus E, Strotmann J and Breer H: Rapid activation of alternative second messenger pathways in olfactory cilia from rats by different odorants. EMBO J 9: 2453-2458, 1990.
5. Reed RR: Signaling pathways in odorant detection. Neuron 8: 205-209, 1992.
6. Fleischer J, Breer H and Strotmann J: Mammalian olfactory receptors. Front Cell Neurosci 3: 9, 2009.
7. Klasen K, Corey EA, Kuck F, Wetzel CH, Hatt H and Ache BW: Odorant-stimulated phosphoinositide signaling in mammalian olfactory receptor neurons. Cell Signal 22: 150-157, 2010.
8. Buck L and Axel R: A novel multigene family may encode odorant receptors: A molecular basis for odor recognition. Cell 65: 175-187, 1991.
9. Parmentier M, Libert F, Schurmans S, Schiffmann S, Lefort A, Eggerickx D, Ledent C, Mollereau C, Gérard C, Perret J, *et al*: Expression of members of the putative olfactory receptor gene family in mammalian germ cells. Nature 355: 453-455, 1992.
10. Spehr M, Gisselmann G, Poplawski A, Riffell JA, Wetzel CH, Zimmer RK and Hatt H: Identification of a testicular odorant receptor mediating human sperm chemotaxis. Science 299: 2054-2058, 2003.
11. Milardi D, Colussi C, Grande G, Vincenzoni F, Pierconti F, Mancini F, Baroni S, Castagnola M, Marana R and Pontecorvi A: Olfactory receptors in semen and in the male tract: From proteome to proteins. Front Endocrinol (Lausanne) 8: 379, 2018.
12. Eisenbach M and Giojalas LC: Sperm guidance in mammals-an unpaved road to the egg. Nat Rev Mol Cell Biol 7: 276-285, 2006.
13. Griffin CA, Kafadar KA and Pavlath GK: MOR23 promotes muscle regeneration and regulates cell adhesion and migration. Dev Cell 17: 649-661, 2009.
14. Pluznick JL, Protzko RJ, Gevorgyan H, Peterlin Z, Sipos A, Han J, Brunet I, Wan LX, Rey F, Wang T, *et al*: Olfactory receptor responding to gut microbiota-derived signals plays a role in renin secretion and blood pressure regulation. Proc Natl Acad Sci USA 110: 4410-4415, 2013.
15. Tong T, Ryu SE, Min Y, de March CA, Bushdid C, Golebiowski J, Moon C and Park T: Olfactory receptor 10J5 responding to alpha-cedrene regulates hepatic steatosis via the cAMP-PKA pathway. Sci Rep 7: 9471, 2017.
16. Weber L, Maßberg D, Becker C, Altmüller J, Ubrig B, Bonatz G, Wölk G, Philippou S, Tannapfel A, Hatt H and Gisselmann G: Olfactory receptors as biomarkers in human breast carcinoma tissues. Front Oncol 8: 33, 2018.
17. Gelis L, Jovancevic N, Veitinger S, Mandal B, Arndt HD, Neuhaus EM and Hatt H.: Functional characterization of the odorant receptor 51E2 in human melanocytes. J Biol Chem 291: 17772-17786, 2016.
18. Weber L, Al-Refae K, Ebbert J, Jägers P, Altmüller J, Becker C, Hahn S, Gisselmann G and Hatt H: Activation of odorant receptor in colorectal cancer cells leads to inhibition of cell proliferation and apoptosis. PLoS One 12: e0172491, 2017.
19. Weber L, Schulz WA, Philippou S, Eckardt J, Ubrig B, Hoffmann MJ, Tannapfel A, Kalbe B, Gisselmann G and Hatt H: Characterization of the olfactory receptor OR10H1 in human urinary bladder cancer. Front Physiol 9: 456, 2018.

20. Leja J, Essaghir A, Essand M, Wester K, Oberg K, Tötterman TH, Lloyd R, Vasmatzis G, Demoulin JB and Giandomenico V: Novel markers for enterochromaffin cells and gastrointestinal neuroendocrine carcinomas. Mod Pathol 22: 261-272, 2009.
21. Wu C, Jia Y, Lee JH, Kim Y, Sekharan S, Batista VS and Lee SJ: Activation of OR1A1 suppresses PPAR-γ expression by inducing HES-1 in cultured hepatocytes. Int J Biochem Cell Biol 64: 75-80, 2015.
22. Kalbe B, Schulz VM, Schlimm M, Philippou S, Jovancevic N, Jansen F, Scholz P, Lübbert H, Jarocki M, Faissner A, *et al*: Helional-induced activation of human olfactory receptor 2J3 promotes apoptosis and inhibits proliferation in a non-small-cell lung cancer cell line. Eur J Cell Biol 96: 34-46, 2017.
23. Vadevoo SMP, Gunassekaran GR, Lee C, Lee N, Lee J, Chae S, Park JY, Koo J and Lee B: The macrophage odorant receptor Olfr78 mediates the lactate-induced M2 phenotype of tumor-associated macrophages. Proc Natl Acad Sci USA 118: e2102434118, 2021.
24. Chung C, Cho HJ, Lee C and Koo J: Odorant receptors in cancer. BMB Rep 55: 72-80, 2022.
25. Cui T, Tsolakis AV, Li SC, Cunningham JL, Lind T, Öberg K and Giandomenico V: Olfactory receptor 51E1 protein as a potential novel tissue biomarker for small intestine neuroendocrine carcinomas. Eur J Endocrinol 168: 253-261, 2013.
26. Almobarak B, Amlani V, Inge L, Hofving T, Muth A, Nilsson O, Johansson M, Arvidsson Y and Elias E: Exposure to nonanoic acid alters small intestinal neuroendocrine tumor phenotype. BMC Cancer 23: 267, 2023.
27. Giandomenico V, Cui T, Grimelius L, Öberg K, Pelosi G and Tsolakis AV: Olfactory receptor 51E1 as a novel target for diagnosis in somatostatin receptor-negative lung carcinoids. J Mol Endocrinol 51: 277-286, 2013.
28. Wang J, Weng J, Cai Y, Penland R, Liu M and Ittmann M: The prostate-specific G-protein coupled receptors PSGR and PSGR2 are prostate cancer biomarkers that are complementary to alpha-methylacyl-CoA racemase. Prostate 66: 847-857, 2006.
29. Maßberg D, Jovancevic N, Offermann A, Simon A, Baniahmad A, Perner S, Pungsrinont T, Luko K, Philippou S, Ubrig B, *et al*: The activation of OR51E1 causes growth suppression of human prostate cancer cells. Oncotarget 7: 48231-48249, 2016.
30. Pronin A and Slepak V: Ectopically expressed olfactory receptors OR51E1 and OR51E2 suppress proliferation and promote cell death in a prostate cancer cell line. J Biol Chem 296: 100475, 2021.
31. Choi EW, Seen DS, Song YB, Son HS, Jung NC, Huh WK, Hahn JS, Kim K, Jeong JY and Lee TG: AdHTS: A high-throughput system for generating recombinant adenoviruses. J Biotechnol 162: 246-252, 2012.
32. Shepard BD, Natarajan N, Protzko RJ, Acres OW and Pluznick JL: A cleavable N-terminal signal peptide promotes widespread olfactory receptor surface expression in HEK293T cells. PLoS One 8: e68758, 2013.
33. Jeong JY, Yim HS, Ryu JY, Lee HS, Lee JH, Seen DS and Kang SG: One-step sequence- and ligation-independent cloning as a rapid and versatile cloning method for functional genomics studies. Appl Environ Microbiol 78: 5440-5443, 2012.
34. Hong JM, Lee JW, Seen DS, Jeong JY and Huh WK: LPA1-mediated inhibition of CXCR4 attenuates CXCL12-induced signaling and cell migration. Cell Commun Signal 21: 257, 2023.
35. Livak KJ and Schmittgen TD: Analysis of relative gene expression data using real-time quantitative PCR and the 2(-delta delta C(T)) method. Method 25: 402-408, 2001.
36. Hague C, Uberti MA, Chen Z, Bush CF, Jones SV, Ressler KJ, Hall RA and Minneman KP: Olfactory receptor surface expression is driven by association with the beta2-adrenergic receptor. Proc Natl Acad Sci USA 101: 13672-13676, 2004.
37. Bush CF, Jones SV, Lyle AN, Minneman KP, Ressler KJ and Hall RA: Specificity of olfactory receptor interactions with other G protein-coupled receptors. J Biol Chem 282: 19042-19051, 2007.
38. Li YR and Matsunami H: Activation state of the M3 muscarinic acetylcholine receptor modulates mammalian odorant receptor signaling. Sci Signal 4: ra1, 2011.
39. Jiang Y, Li YR, Tian H, Ma M and Matsunami H: Muscarinic acetylcholine receptor M3 modulates odorant receptor activity via inhibition of β arrestin-2 recruitment. Nat Commun 6: 6448, 2015.
40. Krautwurst D, Yau KW and Reed RR: Identification of ligands for olfactory receptors by functional expression of a receptor library. Cell 95: 917-926, 1998.
41. Zhuang H and Matsunami H: Synergism of accessory factors in functional expression of mammalian odorant receptors. J Biol Chem 282: 15284-15293, 2007.
42. Li M, Schweiger MW, Ryan DJ, Nakano I, Carvalho LA and Tannous BA: Olfactory receptor 5B21 drives breast cancer metastasis. iScience 24: 103519, 2021.
43. Thomsen MT, Busk M, Zhang D, Chiu CL, Zhao H, Garcia-Marques FJ, Bermudez A, Pitteri S, Borre M, Brooks JD and Nyengaard JR: The olfactory receptor OR51E2 regulates prostate cancer aggressiveness and modulates STAT3 in prostate cancer cells and in xenograft tumors. BMC Cancer 25: 535, 2025.
44. Yang F, Yang J, Zhu C, Ding T, Zhang X and Zhang H: Olfactory receptor OR51B5 suppressed esophageal cancer progression through activates Calcium / N-Ras signaling. Cell Death Dis 16: 450, 2025.
45. Masjedi S, Zwiebel LJ and Giorgio TD: Olfactory receptor gene abundance in invasive breast carcinoma. Sci Rep 9: 13736, 2019.
46. Kajimoto T, Okada T, Yu H, Goparaju SK, Jahangeer S and Nakamura S: Involvement of sphingosine-1-phosphate in glutamate secretion in hippocampal neurons. Mol Cell Biol 27: 3429-3440, 2007.
47. Kajimoto T, Okada T, Miya S, Zhang L and Nakamura S: Ongoing activation of sphingosine 1-phosphate receptors mediates maturation of exosomal multivesicular endosomes. Nat Commun 4: 2712, 2013.
48. Okada T, Nishida S, Zhang L, Ibrahim Mohamed NN, Wang T, Ijuin T, Kajimoto T and Nakamura SI: Constitutive activation of S1P receptors at the *trans*-golgi network is required for surface transport carrier formation. iScience 24: 103351, 2021.
49. Rodriguez-Berriguete G, Fraile B, Martinez-Onsurbe P, Olmedilla G, Paniagua R and Royuela M: MAP kinases and prostate cancer. J Signal Transduct 2012: 169170, 2012.
50. Lorenzo PI and Saatcioglu F: Inhibition of apoptosis in prostate cancer cells by androgens is mediated through downregulation of c-Jun N-terminal kinase activation. Neoplasia 10: 418-428, 2008.
51. Xu R and Hu J: The role of JNK in prostate cancer progression and therapeutic strategies. Biomed Pharmacother 121: 109679, 2020.
52. El-Haibi CP, Singh R, Sharma PK, Singh S and Lillard JW Jr: CXCL13 mediates prostate cancer cell proliferation through JNK signalling and invasion through ERK activation. Cell Prolif 44: 311-319, 2011.
53. Magi-Galluzzi C, Mishra R, Fiorentino M, Montironi R, Yao H, Capodieci P, Wishnow K, Kaplan I, Stork PJ and Loda M: Mitogen-activated protein kinase phosphatase 1 is overexpressed in prostate cancers and is inversely related to apoptosis. Lab Invest 76: 37-51, 1997.
54. Uzgare AR, Kaplan PJ and Greenberg NM: Differential expression and/or activation of P38MAPK, erk1/2, and jnk during the initiation and progression of prostate cancer. Prostate 55: 128-139, 2003.
55. Spehr J, Gelis L, Osterloh M, Oberland S, Hatt H, Spehr M and Neuhaus EM: G protein-coupled receptor signaling via Src kinase induces endogenous human transient receptor potential vanilloid type 6 (TRPV6) channel activation. J Biol Chem 286: 13184-13192, 2011.
56. Gao D, Shen Y, Xu L, Sun Y, Hu H, Xu B, Wang Z and Xu H: Acetate utilization promotes hormone therapy resistance in prostate cancer through neuroendocrine differentiation. Drug Resist Updat 77: 101158, 2024.
57. Wenes M, Jaccard A, Wyss T, Maldonado-Pérez N, Teoh ST, Lepez A, Renaud F, Franco F, Waridel P, Yacoub Maroun C, *et al*: The mitochondrial pyruvate carrier regulates memory T cell differentiation and antitumor function. Cell Metab 34: 731-746.e9, 2022.
58. Cho HJ, Yeo DJ, Yang H and Koo J: Comprehensive transcriptomic analysis reveals cell-type-specific roles of human odorant receptors in glioblastoma and the tumor microenvironment. Int J Mol Sci 25: 13382, 2024.